



## Enhanced thermoelectric properties of Cu doped ZnSb based thin films



Zhuang-hao Zheng<sup>a, b</sup>, Ping Fan<sup>a, \*</sup>, Jing-ting Luo<sup>a</sup>, Guang-xing Liang<sup>a, b</sup>, Peng-juan Liu<sup>a</sup>, Dong-ping Zhang<sup>a</sup>

<sup>a</sup> College of Physics and Energy, Institute of Thin Film Physics and Applications, Shenzhen University, 518060, China

<sup>b</sup> Shenzhen Key Laboratory of Sensor Technology, Shenzhen University, 518060, China

### ARTICLE INFO

#### Article history:

Received 21 December 2015

Received in revised form

22 January 2016

Accepted 25 January 2016

Available online 28 January 2016

#### Keywords:

ZnSb

Cu doped

Thermoelectric thin film

### ABSTRACT

Cu doped ZnSb based thin films were deposited by direct current magnetron co-sputtering. X-ray diffraction results show that the un-doped thin film reveals a single ZnSb phase and it transforms to Zn<sub>4</sub>Sb<sub>3</sub> phase after Cu doped. The material with Zn<sub>4</sub>Sb<sub>3</sub> phase which belongs to R-3c space group crystal will lead to lower thermal conductivity. The Hall effect measurement shows that the samples are P-type semiconductors. The electrical conductivity increases after Cu doped due to the increase of carrier concentration and the improvement in crystallinity. Though the Seebeck coefficient decreases after Cu doped, the ZT value increases from 0.11 to 0.43 with higher electrical conductivity and lower thermal conductivity at room-temperature. The temperature-dependent of ZT value is estimated to be ~1.35 for the thin film with Zn<sub>4</sub>Sb<sub>3</sub> phase by using the bulk lattice thermal conductivity together with the thin film electrical thermal conductivity.

© 2016 Elsevier B.V. All rights reserved.

## 1. Introduction

Thermoelectric materials with high conversion efficiency have attracted much attention in the field of applied physics and materials science in the last few decades [1]. The performance of thermoelectric materials is determined by the dimensionless figure of merit (ZT) which is defined as  $\sigma S^2 T / \kappa$ , where  $\sigma$  is the electrical conductivity,  $S$  is the Seebeck coefficient,  $T$  is the absolute temperature and  $\kappa$  is the thermal conductivity [2]. Zn–Sb binary system is one of the promising P-type thermoelectric materials for low cost thermoelectric application. Such as ZnSb has the ZT value of ~0.6 and Zn<sub>4</sub>Sb<sub>3</sub> has the highest ZT value of ~1.3 [3–6]. The behavior of Zn is the important element that determined the thermoelectric properties of the materials. The excess Zn occupies the lattice interstitial site as the free carrier that will increase the phonon and lead to the increase of ZT [7,8]. However, the thermoelectric properties of Zn–Sb binary compounds are still worse than others thermoelectric materials [9–11]. Further improvement in its properties is vital for its large scale application for practical use. Doping and low-dimension structure are the methods to improve

the thermoelectric properties of thermoelectric materials [12–16]. Cu is an active metal and the physical property is similarity as Zn. In some cases, the Cu will be as the “liquid behavior” and cause a specific change of property [17]. So it might occupy the lattice interstitial site as the behavior of Zn in the ZnSb system and causes the increase of thermoelectric properties. In addition, thin film technique is one of the methods for improving the thermoelectric properties of thermoelectric material due to their stronger quantum confinement effect with low dimensional structure [18–20].

Therefore, in this work, Cu doped ZnSb thin films were deposited by direct current magnetron co-sputtering. The influence of Cu doped on the thermoelectric properties of the thin films was studied.

## 2. Experimental details

Thin film specimens were prepared at room temperature by co-sputtering. High purity (4N) Zn, Sb and Cu targets were used in a DC magnetron sputtering facility with the sputtering angle of 45°. The target-substrate distance was 10 cm. The BK7 glass substrate was chosen for substrate and was ultrasonically cleaned in acetone and alcohol for 10 min. The background chamber pressure was  $6.0 \times 10^{-4}$  Pa and the working pressure was 0.4 Pa with the sputtering gas of Ar. Prior to thin film deposition, a 3-min sputtering

\* Corresponding author.

E-mail address: [fanping308@126.com](mailto:fanping308@126.com) (P. Fan).

cleaning process was performed to remove contaminants on the surface of targets. The sputtering power of Zn, Sb and Cu was 40 W, 24 W and 20 W, respectively. The Zn and Sb sputtered uninterrupted for 30 min and the Cu was sputtered in middle of the co-sputtering process for 2 min and 4 min. The un-doped sample was named S1 and the doped samples were named S2 and S3. All the samples were annealed at 673 K under an Ar atmosphere (440 Pa) for 1 h.

The micro-structure of the thin films was studied by X-ray diffraction (XRD) technique (Bruker D8) with the conventional  $\theta$ – $2\theta$  mode. The composition was performed by energy dispersive spectroscopy (EDS) (Zeiss supra 55). The surface morphology was obtained by atomic force microscope (AFM, CSPM5500). The thickness of the thin films was obtained by using a Dektak3 ST surface-profile measurement system (Rigaku Ultima4). The carrier concentration was measured by Van der Pauw Hall measurements at room temperature (ET9000). The thermoelectric properties of the thin films were measured by the four-probe technique and Seebeck coefficient measurement system (SDFP-I) with the temperature gradient method ( $\Delta K = 15$  K) under air atmosphere. The thermal conductivity was measured by transient hot-wire theory method at room-temperature.

### 3. Results and analysis

The Cu content and carrier concentration of the thin films are shown in Table 1. It can be seen that the Cu content is 2.8% and 4.4%. The carrier concentration of S1 is  $0.20 \times 10^{19} \text{ cm}^{-3}$  and increases after Cu doped. The carrier concentration value of S2 is  $4.14 \times 10^{19} \text{ cm}^{-3}$  which is the most suitable carrier concentration to achieve excellent thermoelectric properties [21]. With the increase of Cu content, the carrier concentration of S3 increases to  $1.27 \times 10^{20} \text{ cm}^{-3}$  which is adverse for thermoelectric materials.

X-ray diffraction patterns of the thin films and the characteristic patterns of ZnSb and  $\text{Zn}_4\text{Sb}_3$  are shown in Fig. 1. The XRD peaks of S1 sample are related to ZnSb phase and few impurity peaks were found, indicating that the S1 is the ZnSb. The main peaks of sample S2 are related to the  $\text{Zn}_4\text{Sb}_3$  phase. Though there are some peaks related to ZnSb phase can be observed from S2, plus on the simulation reveals that more than 80% of S2 is  $\text{Zn}_4\text{Sb}_3$  phase. It is similar to S2, the diffraction peaks of S3 are related to the  $\text{Zn}_4\text{Sb}_3$  plane and no related ZnSb peaks or other impurity peaks can be observed. So it indicates that S3 have single  $\text{Zn}_4\text{Sb}_3$  phase. It can be seen that the sample has change the crystal structure from orthorhombic to hexagonal after Cu doped [3,5,6]. The material with  $\text{Zn}_4\text{Sb}_3$  phase will lead to low thermal conductivity which is at least 2 times less than the ZnSb due to the larger phonon scatter [22]. The lattice parameter of sample S2 is 7.031 Å and shrink to 6.933 Å of S3 based on the highest intensity of (030) diffraction. As the Cu ion is smaller than Zn that the incorporation of Cu atoms might substitute the Zn after the vacancy is filled and expected to result in a smaller lattice constant.

The AFM images of S1 ~ S3 and the grain distribution analysis are shown in Fig. 2. Though there are some humps on the surface of S1, the grains are discrete and varying dimensions which are adverse to the electron transports and might cause the worse of

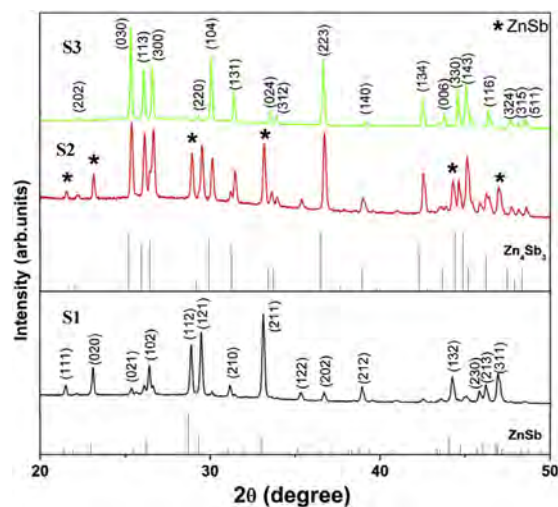
electrical properties. The grains of S2 and S3 become distinct. The surface roughness is decrease from 4.89 nm to 2.39 nm and the average particle size obvious increases after Cu-doped. The big grain size and uniform surface morphology will reduce the grain boundary density which will decrease the electron scattering and lead to the enhancement of the electrical conductivity.

Fig. 3 shows the temperature-dependent of electrical conductivity and Seebeck coefficient of the thin films. As can be seen from the Fig. 3 (a), the positive Seebeck coefficient demonstrates that the thin films are P-type thermoelectric materials which are matched the result of Hall measurement result. The absolute value of Seebeck coefficient decreases after Cu doped. The Seebeck coefficient value reaches to  $174 \mu\text{VK}^{-1}$  and  $87 \mu\text{VK}^{-1}$  at 623 K with the Cu content of 2.8% and 4.4%. They are lower than the value of sample S1. The decrease of the Seebeck coefficient can be attributing to the decrease of the effective mass of the carrier. As can be seen from the Fig. 3 (b), the electrical conductivity of the thin films increases after Cu doped and upgrades with the increase of Cu content due to the tremendous of the carrier concentration and the improvement in crystallinity. For the thermally activated band conduction in a semiconductor film, the dependence of the conductivity on the temperature  $T$  is  $\sigma = \sigma_0 \exp(-E_a/kT)$ , where  $\sigma_0$  is a constant,  $k$  is the Boltzman's constant and  $E_a$  is the activation energy [23]. With this formula and the data in Fig. 3 (b), the activation energy of the samples S1 was calculated to be 463.9 MeV and the average activation energy of S3 was 121.7 MeV. So the thermal band conduction was below the conduction band when the activation energy is decreases and causes the enhancement of electrical conductivity. The electrical conductivity attains to a high value of  $4.41 \times 10^4$  and  $5.46 \times 10^4 \text{ Sm}^{-1}$  at room-temperature. The electrical conductivity of S2 and S3 decreases with the increase of temperature indicates the metallic behavior which can be regarded as the interval Cu provides the main contribution. However, it increases after the temperature reaches to 500 K and the main reason is the intrinsic excitation.

The room-temperature thermal conductivity  $\kappa$  and ZT value of the thin films are shown in Table 2. It can be seen that the thermal conductivity of the thin films reduce from  $1.5 \text{ Wm}^{-1} \text{ K}^{-1}$  to  $0.8 \text{ Wm}^{-1} \text{ K}^{-1}$  after Cu doped, indicates that Cu doped can reduce the thermal conductivity of the ZnSb based thin films. The Cu doped thin film has larger electrical conductivity which leads the bigger electronic part of the thermal conductivity. So the reduce of the thermal conductivity is due to the sharply reduce of the lattice

**Table 1**  
The Cu content and carrier concentration of the thin films.

Sample	Composition (%)			Carrier concentration ( $\times 10^{19}/\text{cm}^{-3}$ )
	Zn	Sb	Cu	
S1	51.9	48.1	—	0.20
S2	51.4	45.8	2.8	4.14
S3	50.5	45.1	4.4	12.7



**Fig. 1.** XRD patterns of ZnSb based thin films.

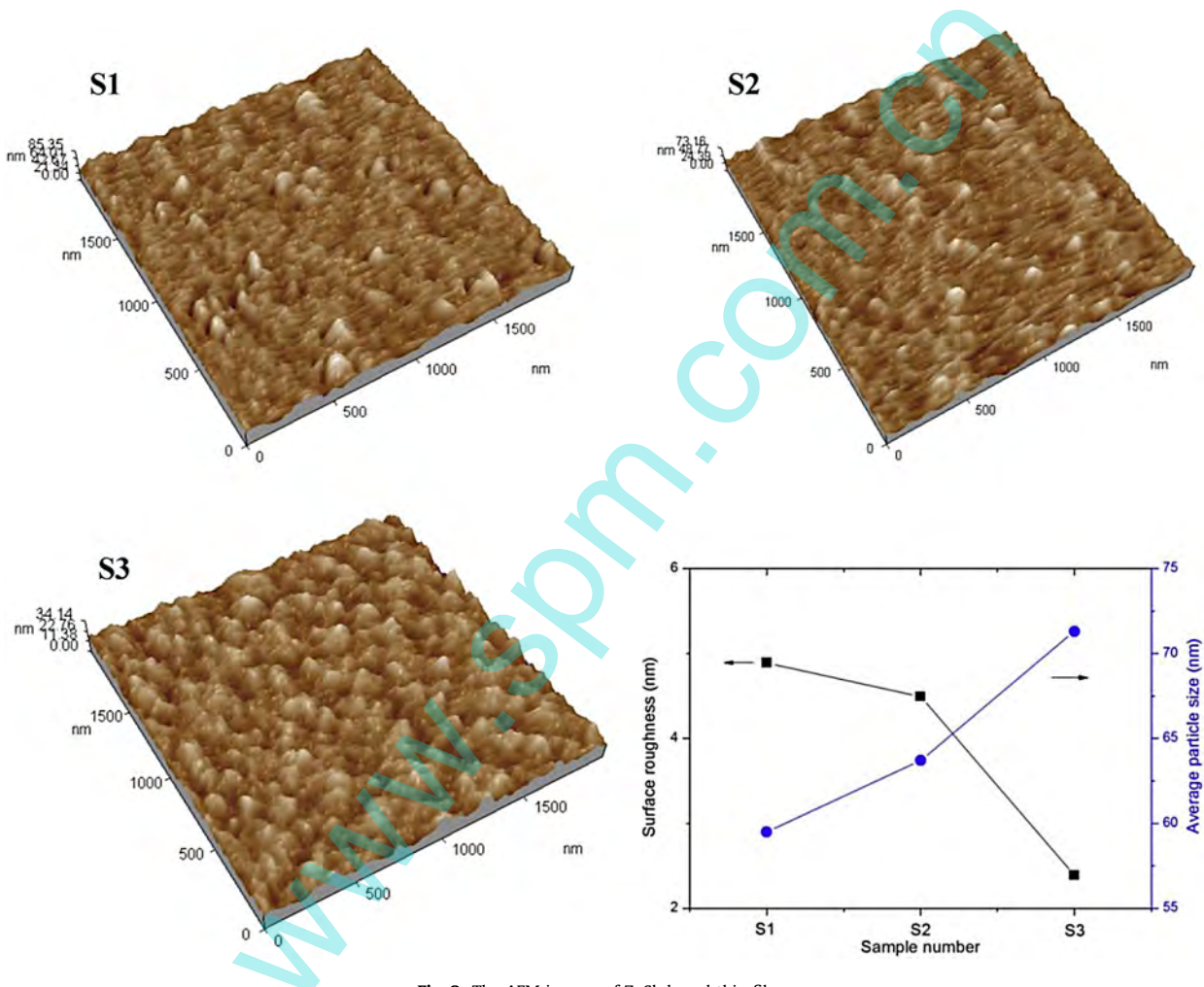
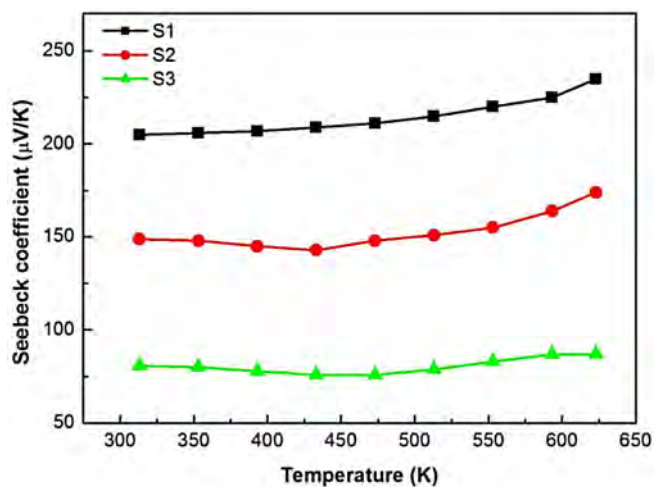
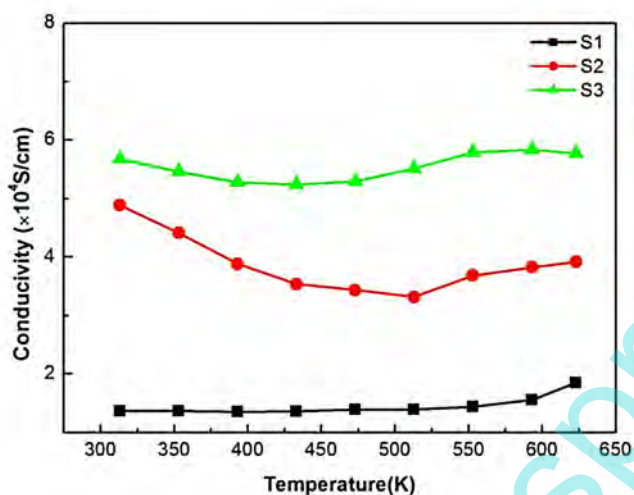


Fig. 2. The AFM images of ZnSb based thin films.



(a)



(b)

Fig. 3. The temperature dependents of Seebeck coefficient (a) and electrical conductivity (b).

thermal conductivity. It can be found that the  $Zn_4Sb_3$  has very lower lattice thermal conductivity than  $ZnSb$ . So the smaller thermal conductivity is due to the change of crystal structure. The ZT value increases from 0.11 to 0.43 and 0.20 when the Cu content is 2.8% and 4.4% which is the great result on the  $ZnSb$  based materials at room-temperature.

Fig. 4 shows the estimated temperature dependents of ZT value for the S1 (un-doped) and S2 (Cu-doped) thin films. To obtain  $\kappa$ ,  $\kappa_e$  was calculated from measured values of  $\sigma$ , and added to literature values of bulk  $\kappa_l$  from the corresponding  $ZnSb$  and  $Zn_4Sb_3$  bulk materials. The highest ZT of the S1 was estimated to be  $\sim 0.39$  and increases to  $\sim 1.35$  of S2 at 623 K. These values are conservatively estimated since the thin films should have a much lower  $\kappa$  due to

Table 2

Room-temperature thermal conductivity and ZT value of the thin films.

Sample	Thermal conductivity ( $Wm^{-1} K^{-1}$ )	ZT value
S1	1.5	0.11
S2	0.8	0.43
S3	0.9	0.20

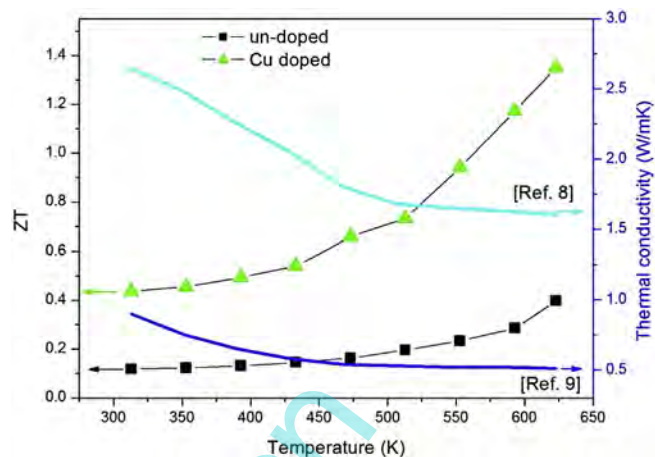


Fig. 4. The estimated temperature dependents of ZT value.

their small crystallite sizes and thus the ZT values would be higher.

#### 4. Conclusions

Cu doped  $ZnSb$  based thin films were prepared with different Cu content. After Cu doped, the electrical conductivity increases and the Seebeck coefficient decreases. The Cu doped thin film with  $Zn_4Sb_3$  phase has lower thermal conductivity compared to the un-doped thin film. As the composite result, the ZT value of the thin film enhanced from 0.11 of un-doped to 0.43 with the Cu of 2.8% at room-temperature and estimated to be  $\sim 1.35$  with the Cu of 2.8% at 623 K. It reveals that Cu doping can improve the thermoelectric properties of the  $ZnSb$  based thin films, which is promising for thermoelectric applications.

#### Acknowledgments

Supported by Special Project on the Integration of Industry, Education and Research of Guangdong Province (2012B091000174), Basic Research Program of Shenzhen (JCY20140418181958500) and Natural Science Foundation of SZU (Grant No. 201418).

#### References

- [1] G.J. Snyder, E.S. Toberer, *Nat. Mater.* 7 (2008) 105–114.
- [2] L.D. Zhao, S.H. Lo, Y. Zhang, H. Sun, G. Tan, C. Uher, C. Wolverton, V.P. Dravid, M.G. Kanatzidis, *Nature* 508 (2014) 373–377.
- [3] L. Bjerg, G.K. Madsen, B.B. Iversen, *Chem. Mater.* 23 (2011) 3907–3914.
- [4] N.L. Kostur, V.I. Psarev, *Sov. Phys. J.* 10 (1967) 21–23.
- [5] M. Liu, X.Y. Qin, C.S. Liu, L. Pan, H.X. Xin, *Phys. Rev. B* 81 (2010) 245215.
- [6] G.J. Snyder, M. Christensen, E. Nishibori, T. Caillat, B.B. Iversen, *Nat. Mater.* 3 (2004) 458–463.
- [7] S.C. Ur, I.H. Kim, P. Nash, *J. Mater. Sci.* 42 (2007) 2143–2149.
- [8] D. Li, X.Y. Qin, *Intermetallics* 19 (2011) 1651–1655.
- [9] D. Wu, L.D. Zhao, S.Q. Hao, Q.K. Jiang, F.S. Zheng, J.W. Doak, H.J. Wu, H. Chi, Y. Gelbstein, C. Uher, C. Wolverton, M. Kanatzidis, J.Q. He, *J. Am. Chem. Soc.* 136 (2014) 11412–11419.
- [10] K. Biswas, J.Q. He, I.D. Blum, C.I. Wu, T.P. Hogan, D.N. Seidman, V.P. Dravid, M.G. Kanatzidis, *Nature* 489 (2012) 414–418.
- [11] J.P. Heremans, V. Jovicic, E.S. Toberer, A. Saramat, K. Kurosaki, A. Charoenphakdee, S. Yamanaka, G.J. Snyder, *Science* 321 (2008) 554–557.
- [12] J.P. Lin, G.J. Qiao, L.Z. Ma, Y. Ren, B.F. Yang, Y.J. Fei, L. Lei, *Appl. Phys. Lett.* 102 (2013) 163902.
- [13] L.D. Hicks, M.S. Dresslhaus, *Phys. Rev. B* 47 (1993) 16631.
- [14] R. Venkatasubramanian, E. Siivola, T. Colpitts, B. O'Quinn, *Nature* 413 (2001) 597.
- [15] M.S. Dresslhaus, G. Chen, M.Y. Tang, R.G. Yang, H. Lee, D.Z. Wang, Z.F. Ren, J.P. Fleurial, P. Gogna, *Adv. Mater.* 19 (2007) 1043–1053.
- [16] L. Bjerg, G.K. Madsen, B.B. Iversen, *Chem. Mater.* 23 (2011) 3907–3914.
- [17] H.L. Liu, X. Shi, F.F. Xu, L.L. Zhang, W.Q. Zhang, L.D. Chen, Q. Li, C. Uher, Tr Day, G.J. Snyder, *Nat. Mater.* 11 (2012) 422–425.



- [18] Y. Sun, M. Christensen, S. Johnsen, N.V. Nong, Y. Ma, M. Sillassen, E. Zhang, A.E. Palmqvist, J. Böttiger, B.B. Iversen, *Adv. Mater.* 24 (2012) 1693–1696.
- [19] L.T. Zhang, M. Tsutsui, K. Ito, M. Yamaguchi, *Thin Solid Films* 443 (2003) 84–90.
- [20] J. Walachová, R. Zeipl, J. Zelinka, V. Malina, M. Pavelka, M. Jelínek, V. Studnička, P. Lošťák, *Appl. Phys. Lett.* 87 (2005) 081902.
- [21] X. Chen, D. Parker, M.H. Du, D.J. Singh, *New J. Phys.* 15 (2013) 043029.
- [22] B.J. Ren, M.A. Liu, X.G. Li, X.Y. Qin, D. Li, T.H. Zou, G.L. Sun, Y.Y. Li, H.X. Xin, J. Zhang, *J. Mater. Chem. A* 22 (2015) 11768–11772.
- [23] K. Niedziolka, R. Pothin, F. Rouessac, R.M. Ayrál, P. Jund, *J. Phys. Condens. Matter* 26 (2014) 365401.

www.spm.com.cn